Thermoreversible gelation of atactic polystyrene: phase transformation and morphology*

R. M. Hikmet†, S. Callister and A. Keller‡
H. H. Wills Physics Laboratory, University of Bristol, Tyndall Avenue, Bristol BS8 1TL, UK
(Received 29 June 1987; revised 22 December 1987; accepted 5 January 1988)

It has been convincingly demonstrated, that thermoreversible gelation of atactic polystyrene (a-PS) is the consequence of liquid–liquid phase segregation arrested by vitrification in accordance with the scheme of Arnauts and Berghmans, in this case for cyclohexanol as solvent. Matrix inversion from a solvated rubbery to a glassy matrix with increasing polymer concentration has been demonstrated with bicontinuous network structures in the intermediate stages, both by inspection of macroscopic consistency and by a scanning electron microscopy (SEM) study of the morphology. The bicontinuous network structure sets in at a highly asymmetric phase composition (low concentrated phase content) which, as substantiated by two-step quenching studies, is associated with passing from the metastable to the spinodal region of the phase diagram. The associated SEM studies allowed the morphological identification of both these regions thus also providing a method for closely defining the metastable–spinodal boundary. This, together with further features of the morphology promises to be potentially relevant to the study of phase transformations and phase morphologies in wider generality. As confined to gelation the present study on a-PS offers, in our opinion, a base for exploring the wider spectrum of thermoreversible gelation effects displayed by polymers in general. In particular, the broadened concept of continuity arising should directly relate to properties and the associated morphologies to the possibility of purposefully created microporous structures; pointers for these are given in this paper.

(Keywords: gelation; polystyrene; liquid–liquid phase segregation; glass transition; morphology)

INTRODUCTION

Gel implies the existence of connectedness through a macroscopic two (or multi)-component system, most readily complied with by a solvated assembly of linked macromolecules. Long chains of chemically jointed units clearly lend themselves to form such a system. Regarding links between chains (network junctions) we shall be concerned with the reversible, hence physical variety, as opposed to the alternative category of permanent, hence chemical junctions. The main issues are: why should a physical gel form at all (i.e. why should a particular solution 'set')?; what is the nature of the junctions?; why can an appropriate gelled system be stable in the solvated state and not proceed to collapse? That a general answer to these questions, and with it a general scheme for physical gelation, have not been forthcoming is due to the large variety of systems displaying physical gelation, each with its own 'personality' preventing comprehensive unification[1].

At one stage it appeared to us[2] that localized interchain crystallization as a junction-forming agency between different chains could provide a unifying theme. While certainly satisfactory for crystallizable polymers, and particularly for those that consist of more than one constituent (copolymers and particularly block copolymers) of differing crystallizabilities along a given chain, there are still problems for a uniform homopolymer, which is also often observed to gel, because such a system would be expected to precipitate eventually (see above). In addition, and chiefly, since the totally uncrystallizable atactic polystyrene (a-PS) was found to gel[3–5], crystallization could not be upheld as a sole and universal basic source for physical gelation any longer (without, however, denying its role where pertinent). In the light of the latter development, we turned to a-PS in our quest for a universal gelation scheme relying on no special source of junction-forming interchain affinity (of which crystallizability is one). We have done so in the belief that if an answer is found then special junction-forming features in their numerous varieties* could then possibly represent additional features overlaying the basic trend.

Short of invoking something as yet completely unknown[3], localized liquid–liquid phase segregation

* Presented at Polymer Physics Group Conference 'Physical Aspects of Polymer Science', Reading, 9–11 September 1987

† Present address: Philips Research Laboratories, Nederlande Philips Bedrijen, BV PO Box 80000 5600 JA, Eindhoven, The Netherlands
‡ To whom correspondence should be addressed

* These embrace junction formation through localized constitutional and conformational features of chains. The former includes ionic bridges, hydrogen bonds, various kinds of complexation, etc., at specific chemical groups; the latter includes features such as intertwining helices that are frequently invoked for gel forming biological molecules[23]. It could also be a combination of both (as most likely in the familiar but still problematic case of gelatin). Also certain conformational changes, when they occur, may promote gelation as reported recently[22,23]. Crystallization could then be regarded as a particular kind of interchain association, which in the predominantly fibrous or micellar version would be primarily and in the chain-folded lamellar variety indirectly (through interlamellar ties), junction, hence gel forming, as in the examples of i-PS[6–8] and PE[9], respectively

0032-3861/88/081378-11$03.00

appeared the most plausible junction-forming process for a-PS (a possibility raised in references 3–5 but dismissed, see later). We can now say that CS_2, used in those investigations, proved to be a most difficult solvent system experimentally. While not denying at this stage that the a-PS–CS_2 system may be special (see later), liquid–liquid phase segregation was favoured when using the more tractable decalin as a solvent in the seminal studies by Arnauts and Berghmans[10]. (The latter results were brought to our attention by Berghmans before publication when our own investigation was undertaken.)

BERGHMANS SCHEME—SCOPE OF WORK

By the Berghmans scheme[10] (as expressed in our formulation) gelation results from localized liquid–liquid phase segregation arrested by vitrification at a stage where the microphases are connected. For this, we consider that there are three requirements which need satisfying: (1) on cooling, the system has to traverse the biphasic coexistence line in the temperature (T)–concentration (c) phase diagram; (2) the polymer-rich phase in the segregated structure should attain the glass transition (T_g) of the corresponding solvent-containing system, when further phase segregation will cease; (3) if at this stage there is mechanical connectedness throughout the system it will 'set' as a gel. Originally such connectedness was envisaged to arise through coil overlap in the initial solution. It follows from the above that $T_{gel} \equiv T_g$, a temperature which, cooling rate determined kinetic effects apart, should be concentration independent. The working of this scheme will be apparent from *Figures 1* and *2*.

Our objective was first to confirm and establish the above conditions using a different solvent, most suitable for work to follow (cyclohexanol), and then to identify and explore the gel morphologies in the light of the above new view point. From this, further issues have arisen (most significantly relating to the mechanism of phase segregation) of wider potential relevance beyond the gel and polymer field, and on the practical plane relating to design and control of porous structures.

Expectations as regards morphology are best expressed through the schematized UCT (upper critical temperature) phase diagram of *Figure 1*, drawn unrealistically symmetrical for a polymer system for easier illustration. Regarding morphology: at low concentrations (inset c_1) the polymer-rich glassy state will be the dispersed phase (drawn shaded) in a solvated matrix (dotted). For high concentrations we would expect the solvated phase to be the dispersed component within a glassy, polymer-rich matrix (inset c_3). When the two phases are commensurate, distinction between matrix and dispersion should blur and both are expected to be continuous, forming interpenetrating networks (inset c_2, the interpenetration cannot be illustrated in two dimensions). These expectations should have consequences which are both obvious and profound for the morphology and properties of the respective gels.

EXPERIMENTAL

Materials

The single polymer used was anionically polymerized narrow distribution a-PS with $M_w = 2.75 \times 10^6$, $M_w/M_n = 1.10$. The solvent used was cyclohexanol.

Methods

The experiment consisted of:

(1) Determination of the phase diagram. This was done by determining the onset of turbidity on cooling in simple laboratory-constructed light scattering apparatus;

(2) Determination of T_g as a function of c. This was done by d.s.c. (Perkin Elmer DSC-2);

(3) Determination of gelation (gel melting) temperature. This was done by the rough (but for the present purpose adequate) method of observing the cessation (for setting) or onset (for melting) of fluidity by tilting a test tube. The melting point of the gel was found more reproducible than the setting temperature; ignoring possible hysteresis effects this was considered in the following.

(4) Morphology. Scanning electron microscopy (SEM) was used on dried specimens. In order to preserve the expanded internal structure as far as possible the solvent was removed by freeze drying. It was found subsequently that this was strictly necessary only for the most dilute systems, otherwise exchange for a more volatile solvent followed by evaporation sufficed, a point to acquire physical significance (see later). Subsequently, an internal surface was exposed, metal coated (ensuring as much unobstructed coating as possible) and examined by SEM. Charging coupled with mechanical instability of the often fragile three-dimensional systems could pose serious problems.

(5) Pre-gelling solution state. Some tentative light scattering examinations were performed to examine the solution below the coexistence curve but above the T_g tie-line. A Sophica instrument was employed.

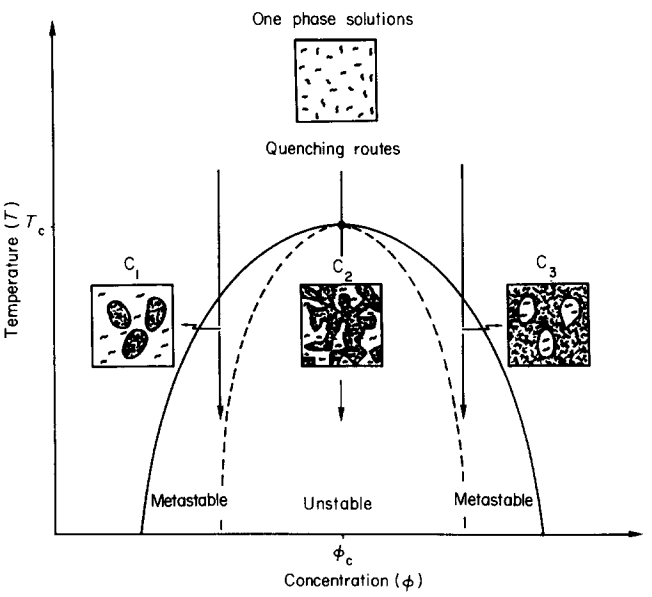

Figure 1 Schematic UCT phase diagram illustrating the expected variation in gel morphology with concentration, c. A dispersed polymer-rich glassy phase in a solvated matrix at low c (inset c_1), a dispersed solvated phase in a glassy matrix at high c (inset c_3) and bicontinuous interpenetrating networks at intermediate c (inset c_2)

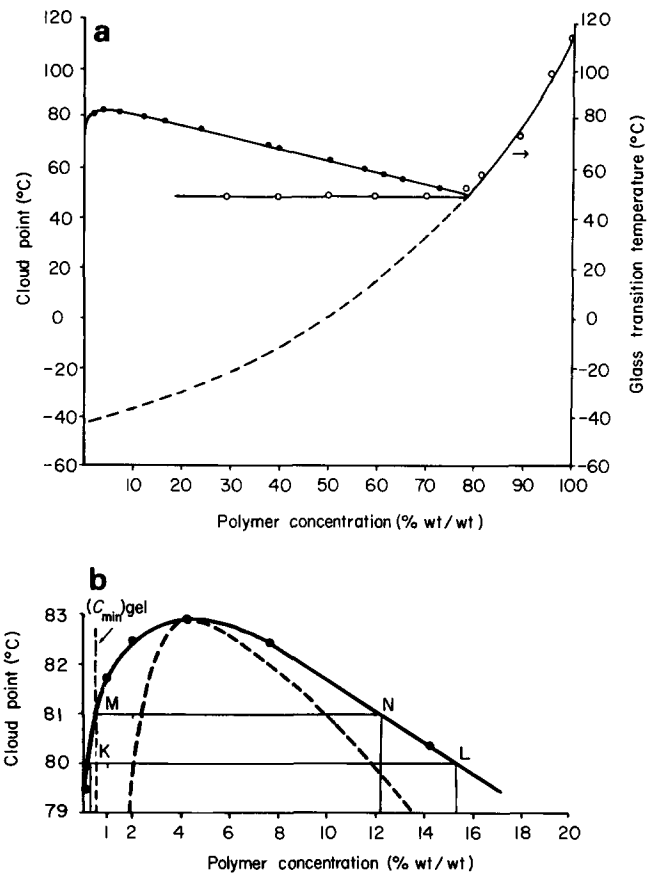

Figure 2 (a) Phase diagram for the atactic polystyrene/cyclohexanol system $M_w = 2.75 \times 10^6$ depicted in relation to the glass transition curve (the broken line is a theoretical extrapolation, see text). (b) Enlarged detail of (a) about the commensurate point. The boundary (c_{min})gel, and the 80 and 81°C tie lines are shown. The end points of the two tie lines drawn KL and NM, respectively, with the concentrations at 1 and 2% marked along the respective tie lines, together with the points along the coexistence curve relate to experiments described in the text. The heavy broken line represents the expected (see text) spinodal boundary

RESULTS AND DISCUSSION

The phase diagram

The biphasic coexistence curve is shown in *Figure 2a*, with enlarged detail in *Figure 2b*. As expected, it is of the UCT type and highly asymmetric with UCT at 83°C, and the rest of the 'useful' portion of the curve being between 40°C and 83°C.

Glass transition, T_g

Figure 3 shows thermograms used to determine T_g, where a glassy polymer (or gel) is being heated. T_g, readily identifiable, drops with decreasing polymer concentration becoming invariant below 78%. The latter feature is in accordance with Arnauts and Berghmans[10] who used a different solvent, and is depicted in relation to the phase diagram in *Figure 2a*. Here the dashed line is a theoretical extrapolation below 78% (for theory see ref. 11) for the, in practice unrealizable, situation that phase segregation is suppressed and the solution stays homogeneous. The point at $c = 0$ would be the T_g of the pure solvent.

Gelation

Gel setting occurred over the whole c range from below 1% up to 78%. The low c gelation limit was found to lie between 0.5% and 0.65%. The lower concentration limit (c_{min}) gel is indicated in *Figure 2b*. Beyond 78% the setting effect was indistinguishable from conventional vitrification.

The gel setting temperature was cooling rate dependent. Using the gel melting temperature instead, this was found to be close to 50°C, i.e. close to T_g, over the whole c range (even if the experimental uncertainties were of different kinds at the dilute and highly concentrated end). With fluidity setting in turbidity remained on further heating, disappearing only sharply at the coexistence boundary of *Figure 2*, which shows up also in the thermograms (as a second, higher temperature step in the 50 and 29% traces in *Figure 3*).

Gel features and morphology

Phase compositions. The gels selected for further study were from solutions of 1, 2, 4, 16 and 57%. The proportions of the two phases, polymer-rich and polymer-poor, can be determined from the phase diagram by the lever rule. When applying to $T_{gel} \equiv T_g$, the phase compositions were found to be as given by *Table 1*.

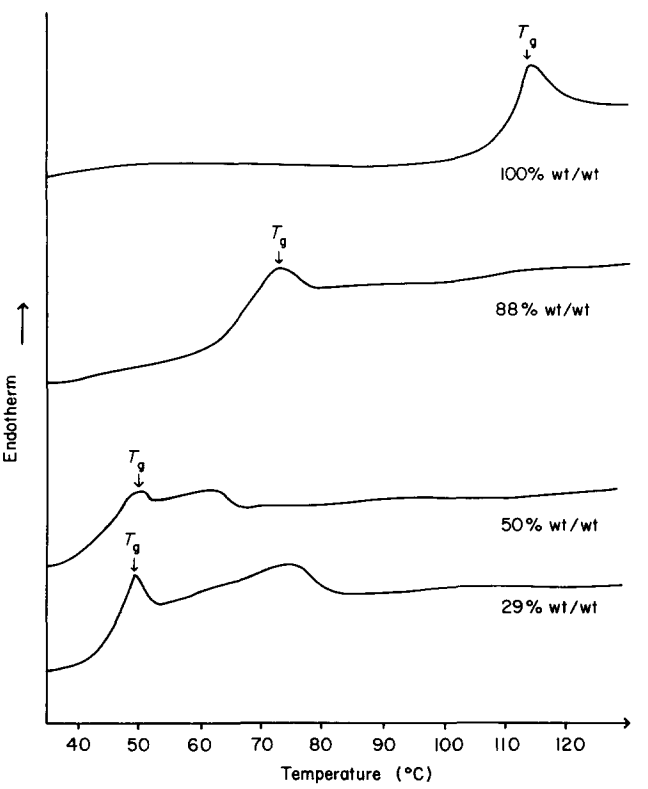

Figure 3 Examples of thermograms used to determine T_g

Table 1 The ratio of the polymer-rich to the polymer-poor phase calculated using the lever rule at the glass transition temperature, i.e. the phase composition ratio as a function of inital solution concentration

Initial solution concentration (wt/wt) (%)	Phase composition ratio (%)
1	1.3
2	2.6
4	5.4
14	21.8
57	271.0

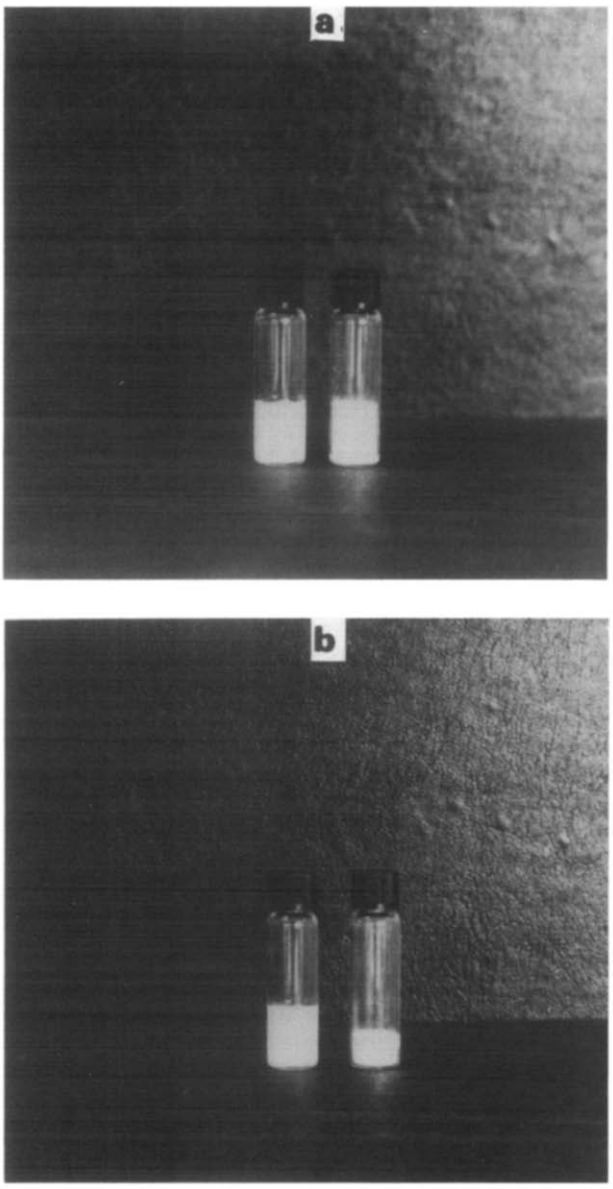

Figure 4 1% and 4% gels before (a) and after (b) solvent removal showing macroscopic shrinkage of the 1% sample

Macroscopic features. The gels obtained from different concentrations differed as regards macroscopic behaviour. Thus, most apparently even by inspection, all gels from 4% concentration and upwards retained their overall macroscopic dimension on solvent exchange and drying, while the 1% gel shrunk on solvent removal as shown by *Figure 4*. The latter shrinkage showed some (but by no means full) reversibility. Correspondingly, the gels displayed some gross differences also on mechanical handling. The 1% gels, even if very weak, were more stretchable and elastic than the rest. While quantification is clearly required, both the shrinkage and handling behaviour suggest a rubbery matrix below 4% and a glassy matrix at and above 4% (with 2% at the borderline, see later) a major conclusion, even in this rudimentary stage, to be pursued in the following SEM examination.

SEM morphology. Characteristic SEM photographs of gels obtained from different solutions on rapid cooling directly from the solution state are shown in *Figures 5–9*. *Figure 9* of the most concentrated solution of the series, is a clear case of the dilute phase forming droplets (seen as holes left by the solvent as it had evaporated) within a glassy matrix in accordance with expectations (insert for c_3, *Figure 1*). *Figure 5* shows the most dilute solution and is seen to consist of strings of small beads ($\sim$ 1–2 μm). We interpret this as arising from a gel consisting of glassy

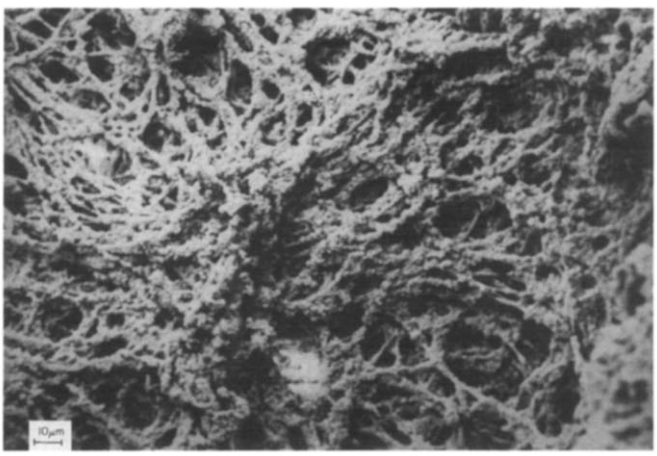

Figure 5 Scanning electron micrograph of a 1% gel sample directly quenched prior to freeze-drying

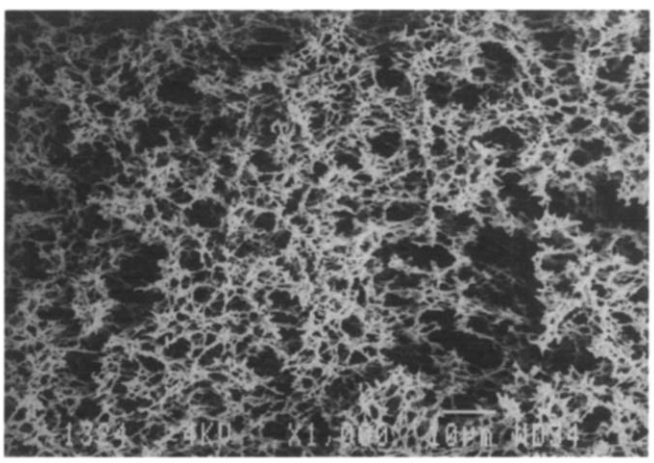

Figure 6 Scanning electron micrograph of a 2% gel sample directly quenched prior to freeze-drying

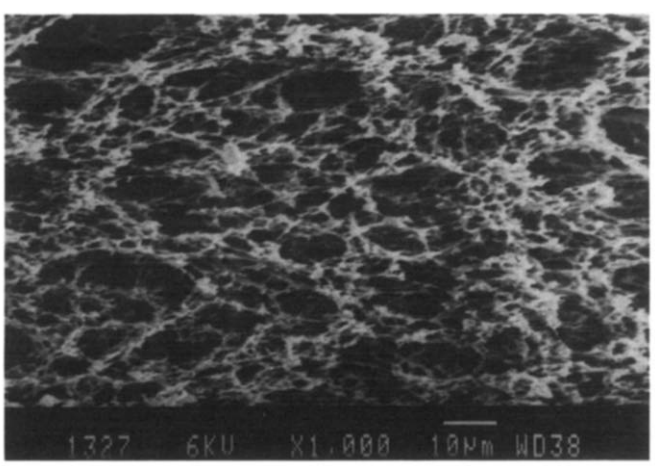

Figure 7 Scanning electron micrograph of a 4% gel sample directly quenched prior to freeze-drying

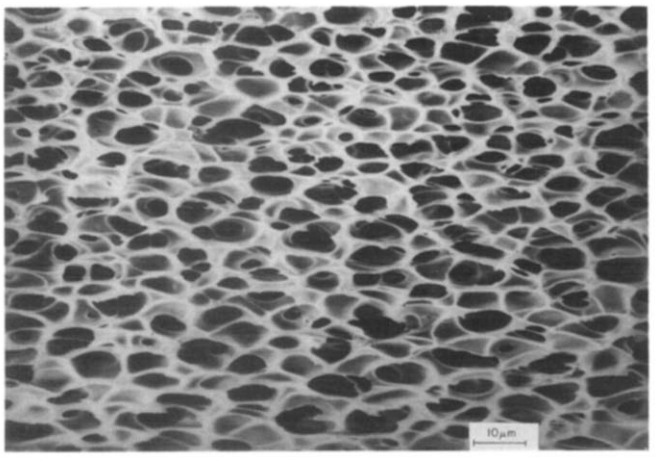

Figure 8 Scanning electron micrograph of a 16% gel sample directly quenched prior to freeze-drying

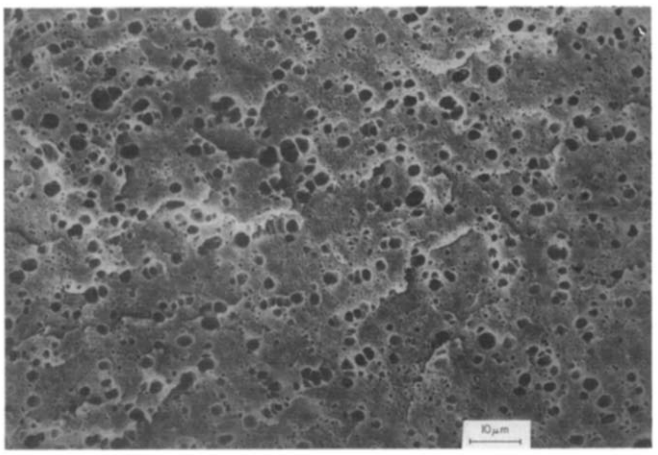

Figure 9 Scanning electron micrograph of a 57% gel sample directly quenched prior to freeze-drying

beads in a solvated matrix (insert for c_1 in *Figure 1*), i.e. the inverse of *Figure 9*, but affected by collapse on solvent removal. If the gel structure is as sketched, together with connecting elements (*Figure 10*), such collapse must take place even on applying freeze drying, as reflected by the macroscopic shrinkage in *Figure 4*, because the initially solvated connecting molecules cannot remain free standing individually, even in the (macroscopically) vitrified state. The molecules will need to bunch, which could account for the string-like features seen. The plausibility of this (even if not automatically for the apparently rather large scale (tens of microns) mesh structure constituted by the web of strings) interpretation for *Figure 5* will be borne out by what follows.

Between the two extremes of dispersed glassy beads and dilute solution droplets, are the bicontinuous structures from the intermediate concentrations. *Figure 8* is like *Figure 9* but is from the intermediate concentrations, and shows much larger holes; it corresponds to a rigid foam. The continuity of the glassy phase is obvious. Whether the dilute solution phase (cavities in the SEM) form a closed or an open, hence interconnected, structure cannot be assessed with certainty from the photograph. By selecting suitable concentrations either state should be realizable.

The gel structures from the 2% (*Figure 6*) and 4% (*Figure 7*) concentrations are different from the above, and are not ready extensions of the structures seen in the dilute and/or concentrated extremes, a fact to which we shall assign special significance later. The glassy phase, which gives it overall (even if fragile) rigidity, appears like a three-dimensional, rather spiky wire network with intervening empty spaces (the original dilute phase) also displaying continuity. Thus, here the combination of dilute and concentrated phases represent bicontinuous networks. The intermediate nature of these structures (inset c_2, *Figure 1*) is not unexpected *per se*, yet the establishment of continuity in the concentrated phase, even at phase composition ratios as low as 2.6 and 5.4% (*Table 1*), is unexpected, and so is the distinct character of the morphology.

To summarize, we see the full range of morphologies which, while expected a priori (insets in *Figure 1*), were realized in a predesigned, systematic manner, relying on the Berghmans scheme with certain unusual features in the intermediate stages which deserve further attention.

Two-stage quenching. Mechanism of phase segregation

Here we refer to the tentative metastable-spinodal boundary line in *Figure 2b*. While the actual position in our system is not known it is expected with certainty that: (1) at a concentration corresponding to the apex of the cloud point curve (UCT), which is at 4% polymer, we are within the spinodal region at all temperatures below the UCT; (2) at other concentrations very closely inside the cloud point line we should be in the metastable region where phase segregation is via nucleation.

From the shape of the coexistence curve, it is reasonable that (2) should hold for, say, 1% concentrations at temperatures several degrees below UCT, and down to T_g. In appearance, (2) is expected to be manifest by droplets. The string of beads structure in *Figure 5* is certainly consistent with this. In contrast, for (1), the visual images are not readily predictable as it is not obvious a priori how a structure consisting of continuous and periodic density fluctuations in all three dimensions (attributes of the initial stages of spinodal decomposition) would look if they could be preserved and made visible. In addition, the latter will depend on the stage at which the spinodal decomposition (i.e. the position along a given horizontal tie line) becomes arrested, not to mention the possible accompanying preparative artefacts. Nevertheless, the different character of the phase-segregated structure in the 4% case (*Figure 7*), where we know that the system must have passed through the spinodal region, implies that the image seen could be at least a reflection of spinodal

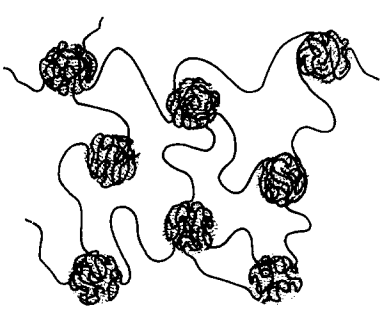

Figure 10 Sketch of the 1% gel structure prior to solvent removal, showing molecularly connected glassy beads in a solvated matrix

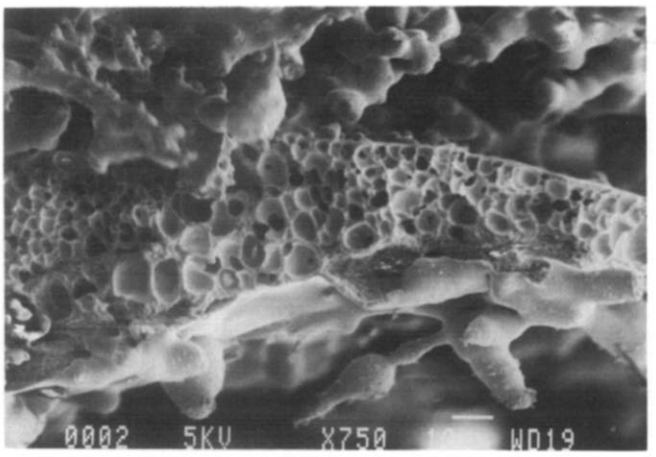

Figure 11 Scanning electron micrograph of a 1% gel sample stored at 80°C for 30 min prior to freeze-drying

decomposition, if not the spinodal structure itself. If so, this would apply, by similarity in appearance, also to the 2% case in *Figure 6*.

The above assignment of observed structures to nucleation and spinodal mechanisms, respectively, gains further support through some two-step quench experiments. Here solutions of different concentration are first held at temperatures below the cloud point curve but above the gelation temperature (i.e. T_g), so as to induce phase segregation without the arresting effect by vitrification. If allowed to completion, this should lead to two macroscopically defined phases separated by a single phase boundary, which could always be observed after sufficient holding time. For shorter times the separated phases will be in varying states of dispersion or coalescence. In this latter situation we cannot be certain of how far the final equilibrium composition has been attained or approached within each phase (i.e. the exact position along a given tie line) at the time of quenching to T_g.

In the following some spot tests are reported, which are revealing, particularly with reference to *Figure 2b*.

Let us consider cases where the phase segregation at the storage temperature narrowly straddles the critical gel concentration ((c_{min}) gel), and then consider cases which straddle the spinodal boundary. The former is known from the preceding experiments while the latter is merely inferred.

The storage temperature was 80°C and the concentration was 1%, a concentration which on single-stage quenching gave the gel in *Figure 5*. This system in its entirety ceased to gel on quenching to T_g for all storage times beyond 5 min, by which time phase segregation became apparent. However, on quenching to T_g after 30 min storage the polymer-rich phase, which had become macroscopically distinct, displayed gelation while the polymer-poor phase remained fluid. The reason for this will be apparent when considering the tie line KL in *Figure 2b*. Here the dilute phase end K, corresponding to $c = 0.25\%$, is below the gelation limit (c_{min}) gel which is 0.6%. Thus, by producing phase separation at 80°C we removed the gelling ability of the dilute phase which, in the case that this is still the matrix phase of a dispersed system, means gelation of the system as a whole. At the high concentration end (L) the concentration is 15%, i.e. above (c_{min})gel. Consequently the phase can now gel on its own, as observed. The morphology of this latter gel, as examined by SEM, is shown in *Figure 11*. As seen, it has a foam structure rather like that shown in *Figure 8* which is from a 16% solution quenched in a *single* step to below T_g. We see that once phase segregated, each component will gel (or not gel) on quenching to T_g, just as an initially single phase solution of the corresponding concentration would do and, in the case of gelation, with the corresponding morphology.

Figure 12 is the same system as in *Figure 11* but quenched to T_g after the shorter holding time of 8 min. It shows large latex type spheres: this would be expected from nucleated phase segregation but at an earlier stage, before coalescence. In addition, as a special point of interest, the spheres are decorated by a fine lace filigree. It is tempting to surmise that this is a remnant of the polymer-poor phase whose concentration has fallen below the gelling limit of 0.6% and can only form kinds of finite networks, insufficient to produce a fully connected structure. (If so, this would be a notable way of making such gel precursor structures visible.) There are faint indications of this lace filigree also in *Figure 11*, but in *Figure 12* the effect is much more pronounced. This invites the suggestion of a less complete partitioning within the segregated phases at the earlier stage of *Figure 12*, which would mean that composition K is not yet fully achieved in the dilute phase. This in turn means that the polymer concentration therein should be closer to (c_{min})gel in *Figure 12* than in *Figure 11*, hence the more pronounced gelation precursors in the former.

The above is reinforced by *Figure 13* which corresponds to a storage time of 30 min at the slightly higher temperature of 81°C with a 2% solution. Again, we see a well developed lace filigree, in this case, however, decorating a concentrated phase, which now is in an advanced stage of coalescence. This could follow from the fact that at 81°C the coexistence boundary will be very close to (c_{min})gel (*Figure 2b*), hence on quenching to T_g incipient gelation could occur in the dilute phase even after complete compositional phase segregation.

Next, let us consider a 2% concentration and the still slightly higher storage temperature of 82°C. The system gels even after the longest holding time (30 min), which produces turbidity, on quenching to T_g. Even if there still is a slight amount of supernatant sol, the system is still of

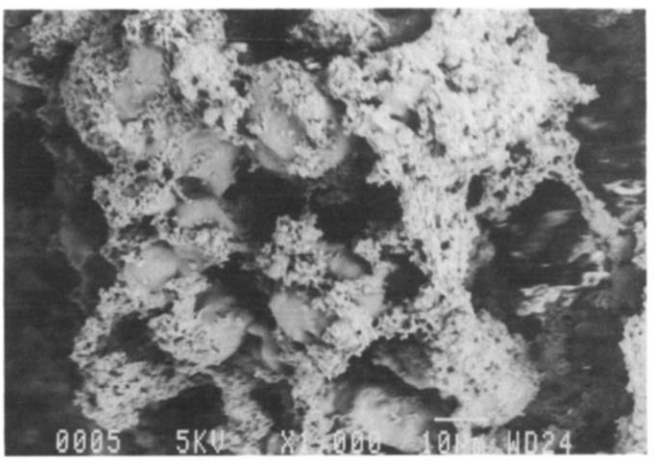

Figure 12 Scanning electron micrograph of a 1% gel sample stored at 80°C for 8 min prior to freeze-drying

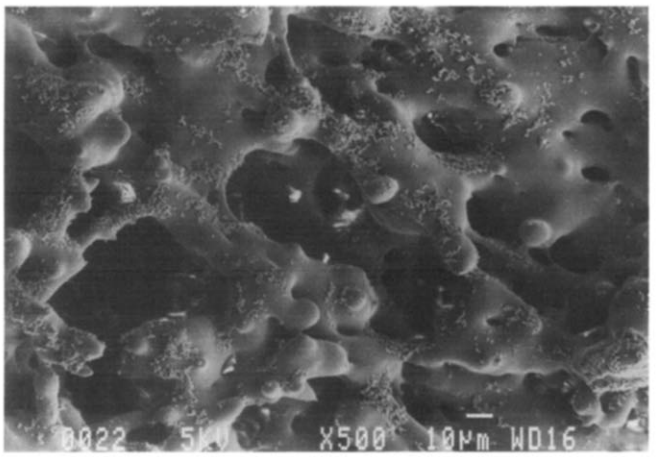

Figure 13 Scanning electron micrograph of a 2% gel sample stored at 81°C for 30 min prior to freeze-drying

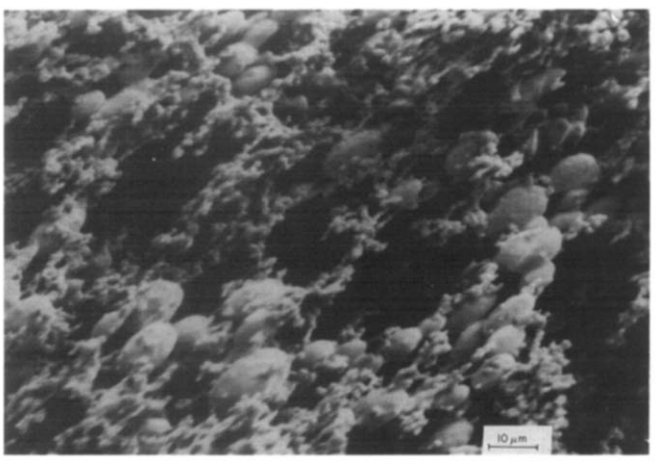

Figure 14 Scanning electron micrograph of a 2% gel sample stored at 81°C for 5 min prior to freeze-drying

overall gel character when compared with the fluid state of a sample having had identical storage times at the lower temperatures of 80 and 81°C. While it may appear contrary to intuitive expectations, as the driving force towards phase segregation is greater at the lower temperature, this observation is in fact consistent with the fact that at the dilute end of a corresponding 82°C tie line $c = 1\%$, i.e. larger than (c_{min})gel. So far this experiment completes the straddling of (c_{min})gel.

As a next stage, we consider the spinodal boundary. *Figure 14* is a SEM for a 2% sample held at 81°C for 5 min. It reveals a two-component morphology. The first consists of 10 μm spheres (or rather ellipsoids, we do not comment on the possible reasons for the distortion). These are like the initially unconnected drops of the polymer-rich phase (inset c_1 in *Figure 1*) and are thus clearly products of nucleation. We maintain that these formed during storage at 81°C corresponding to (or approaching) the concentration pertaining to tie end N. The second component is a network of fine strings of beads ($\sim 1\,\mu$m). As seen, it closely resembles the gel structure from a 1% solution obtained by direct quenching, when it is the only structural element present (*Figure 5*). We maintain that this structure, corresponding to the gel-forming component, arises on quenching and originates from the dilute phase product of the phase segregation at 81°C. Indeed, the concentration at M is close to 1% such as pertains to *Figure 5*. The large ellipsoids adhere to this network and are supported by it. Both components are consistent with having arisen through nucleation, and are distinctly different from the spiky network structure given by the same initial concentration on single-stage quenching (*Figure 6*). The implication seems clear: at 81°C the 2% solution is within the metastable, and at 50°C (T_g) it is within the spinodal region. It follows, that by passing from 81 to 50°C we have crossed the spinodal boundary which allows the latter to be closely defined. Clearly, by using smaller temperature intervals still closer definition should be possible thus providing a method for identifying spinodal boundaries in wider generality (on the assumption that the presently adopted visual criterion applies).

Next it remains to be seen how the 4% solution, which is expected to remain within the spinodal region throughout, responds to storage. Quenching to T_g after 5 min at 81°C (a treatment which has produced drastic effects previously) produced no change compared with one-stage quenching (*Figure 7*) and will thus not be illustrated separately. Nevertheless, slow cooling from above the UCT, while retaining the overall spiky wire network structure, produced noticeable coarsening (*Figure 15*) (which incidentally has led to greater mechanical stability in the electron beam, hence to crisper image). This coarsening was promoted further by more prolonged isothermal storage above T_g; *Figures 16* and *17* show two consecutive stages. As seen, the spikes of the network develop into sheets while the overall network character is retained even after storage times which for 1 and 2% have produced near complete phase segregation (*Figures 11* and *13*). As seen, the differences are dramatic.

To sum up, on the basis of visual images we conclude that for $c = 1\%$ we are always in the metastable region, for $c = 2\%$ we may be either in the metastable or spinodal region according to temperature, while for 4% we are in the spinodal region throughout. The spinodal-based structures (for qualifications, see later) are much more stable against further transformation, but unless interrupted by vitrification, complete separation into two macroscopic phases will eventually occur.

In conclusion, the two-step quench experiments have provided strong support to the postulated distinction between nucleated and spinodal phase segregation through visual images of the freeze-dried gel. They have

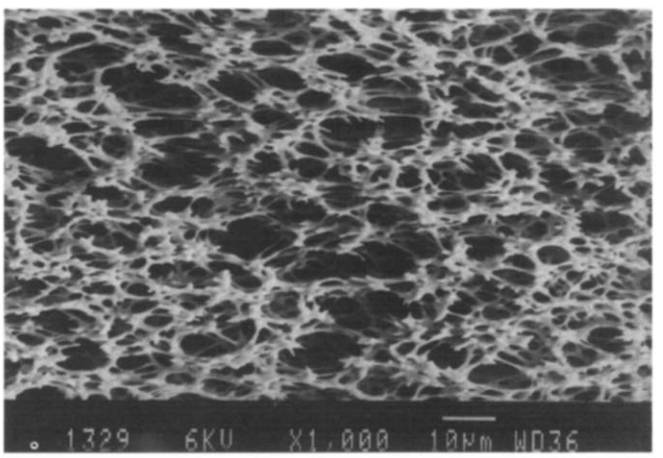

Figure 15 Scanning electron micrograph of a 4% gel sample slowly cooled prior to freeze-drying

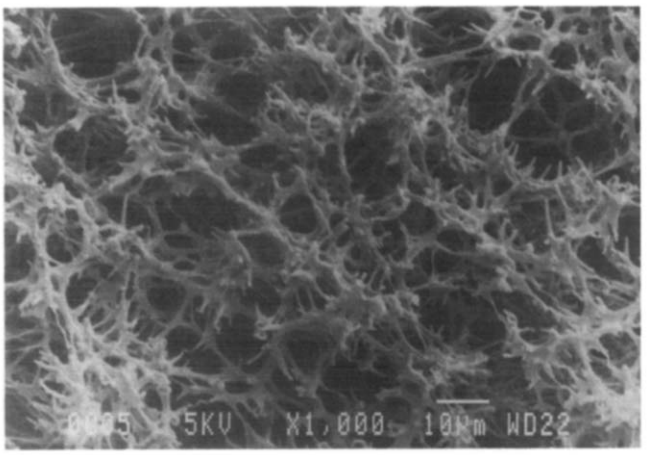

Figure 16 Scanning electron micrograph of a 4% gel sample stored at 81°C for 30 min prior to freeze-drying

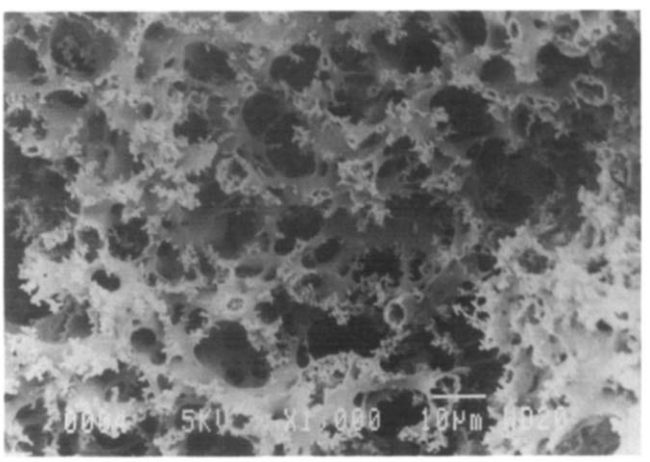

Figure 17 As for *Figure 16* but in a more advanced stage of 'ripening'

demonstrated the role and consequences of a lowest critical gelation concentration, and provided strong support for the phase segregation induced gelation mechanism[10].

The fact that storage above T_g has produced meaningful effects provides justification for the preceding single-stage quenching experiments. More explicitly, the gels obtained by direct quenching cannot be significantly affected by the thermal pathway during a usual cooling experiment with a duration of tens of seconds, and are thus representative of the gelation for the particular initial concentrations involved. (If it were otherwise no clear distinction between the stages of cooling could be made.)

Light scattering. A preliminary test

Predictions of the Cahn–Hilliard theory for spinodal decomposition[12] were tested for the 4% solution in the temperature range 75–60°C, i.e. below the critical point within the spinodal, but above the gel temperature (~50°C), the range being confined by the time scale of the development of the turbidity. According to theory

$$I(q,t)=I(q,0)\exp[2R(q)t] \tag{1}$$

Here R, the rate is given by

$$R(q)=-Mq^2\left[\left(\frac{\partial^2 f}{\partial c^2}\right)+2Kq^2\right] \tag{2}$$

where M=mobility, K=gradient energy coefficient, f=free energy of mixing and c=concentration. The apparent diffusion coefficient $\tilde{D}$ is defined by $\tilde{D}=M(\partial^2 f/\partial c^2)$ and q_m, the wave number corresponding to the highest growth rate, is given by

$$q_m=\frac{1}{2}\left[-\left(\frac{\partial^2 f}{\partial c^2}\right)\frac{1}{K}\right]^{1/2} \tag{3}$$

The scattered intensity I was recorded as a function of time (t) at different scattering angles (θ). As shown by *Figure 18* the $\log I$ vs. t plots for a given q ($q=(4\pi/\lambda)\sin(\theta/2)$) are straight lines. This conforms with expectations from equation (1) thus corroborating the assertion of a spinodal mechanism.

According to theory[13,14], q_m identifies the dominant wavelength λ in the spinodal decomposition, obtainable through plots of $R(q)/q^2$ vs. q^2, where $R(q)$ is extracted from plots such as *Figure 18*. The values for λ (together with $\tilde{D}$) obtained were within 44–50 nm for the temperature range in question (*Table 2*). (It is to be noted that with visible light we are within the spinodal peak, i.e.

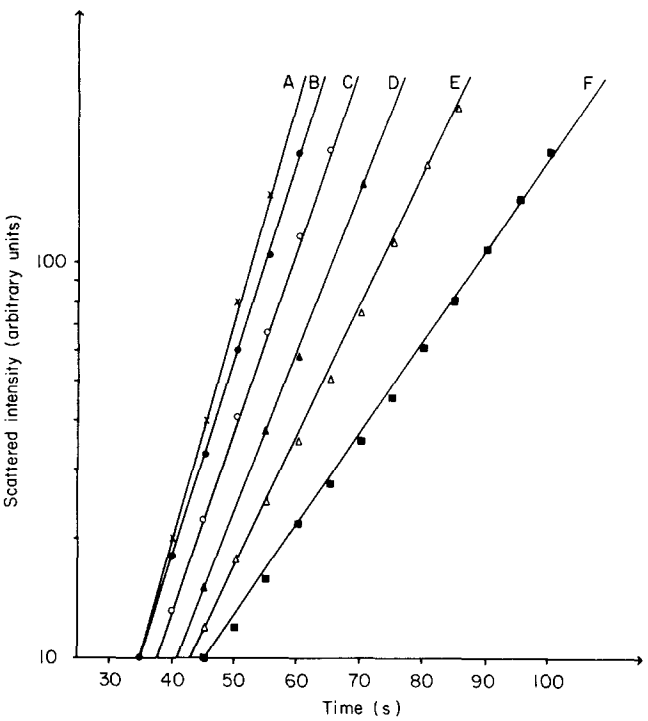

Figure 18 Plots of scattered intensity vs. time for a 4% solution quenched to 75°C at various scattering angles. The slope at a given q value equals twice the growth rate $R(q)$. Values of q: A, 1.99×10^7; B, 2.17×10^7; C, 2.39×10^7; D, 2.59×10^7; E, 2.77×10^7; F, 2.93×10^7

Table 2 Predicted (see text) values of the dominant wavelength λ in the spinodal decomposition and the apparent diffusion coefficient $\tilde{D}$ for various temperatures in the range of interest (i.e. $T_g \rightarrow T_c$)

Temperature (°C)	$\tilde{D}$ ($m^2\ s^{-1}$)	λ (nm)
60	3.9×10^{-16}	48.4
65	3.4×10^{-16}	45.0
70	2.8×10^{-16}	44.6
75	2.3×10^{-16}	43.8

only along the rising portion of the $I(q)$ vs. q curve for such a small structure feature throughout.)

Structures seen in the SEM images, as resolved with the magnification used, are much larger than values in *Table 2*. Hence, they are not likely to correspond directly to the spinodal structures revealed by light scattering, even when allowing for the lower temperature involved in gelation and for possible collapse features during drying. Rather, they represent later stages in the segregation process which are still distinctly related to spinodal decomposition but in a 'ripened' form.

FURTHER ISSUES

The principal issues for discussion have already been developed through the presentation of the experiments. Several additional points nevertheless arise.

Critical minimum gel concentration ($(c_{min})gel$)

The value of ~ 0.6 for (c_{min})gel observed may be compared with c^* conventionally used to characterize the lower limit of chain overlap. For the same polymer, i.e. a-PS $M_w = 2.75 \times 10^6$, this has already been discussed in a different context in references 15 and 16, where a calculated range of 1–5% (depending on numerical factors adopted) and experimental measurement (by neutron scattering) of 5% was quoted, under θ-conditions. Our present value pertaining to gelation would thus lie below c^* slightly or significantly, depending on the c^* value within the above range. For our gelation we are in fact below the θ-temperature, hence the coil size must be still smaller. As argued in references 15 and 16, for a given coil there is a finite segment density well outside the R_g (radius of gyration) conventionally used to define c^*, and we can thus expect some coil overlap (see ref. 16) for molecules which are more widely separated than R_g. Accordingly, what should matter for a particular effect is the segment overlap density required for it. For the case of gelation this is somewhat lower than for a centre of mass separation of $2R_g$ under θ-conditions. For a full test the molecular weight dependence would need to be explored, and work is currently in progress.

Relation to previous works on gelation

A few items relevant to the present work are now discussed, with no attempt to give a comprehensive report, which would require a review by itself.

a-PS. The previous pioneering work on a-PS gels[3] dismissed phase segregation as a possible source, as it claimed that gelation could set in above the coexistence curve. From our present work (and ref. 10) this is clearly not so. However, in reference 3 the prominent gelling systems used CS_2 as solvent. From our own experience with CS_2, the inconveniently low gelling temperatures and high volatility of the solvent apart, the refractive index of polymer and solvent are so close that identification of a coexistence curve is difficult, which would result in an underestimation of the cloud point temperatures. Even so, the possibility that the a-PS–CS_2 system is different outside the Berghmans scheme remains an issue needing further investigation.

i-PS. Our involvement in physical gelation originates from crystallization studies on i-PS solutions in the course of which the systems were seen to gel[6–8]. These gels were found to be crystalline by X-ray diffraction (with some intriguing novel crystallographic and chain conformational features) which led us to attribute the gelation itself to crystallization. In the light of more recently gained knowledge that a-PS can also gel, via liquid–liquid phase segregation, a reassessment of previous work on i-PS is now required. We stress that all the effects reported previously connected with crystallinity (such as two different crystal structures, complex composite morphologies) can be regarded as firmly established. The presently arising issue is whether the prime source of gelation in the crystallizable i-PS is liquid–liquid phase segregation, or the crystallization itself, the latter having been our previous conclusion. Clearly, in the light of the present work on a-PS, gelation by liquid–liquid segregation should at least be possible. If so, crystallization could then follow, possibly first in the polymer-rich phase. Alternatively, in i-PS each gel-forming process, liquid–liquid and liquid–crystal, could occur according to circumstances.

Gelation crystallization. Wider issues and relevant precedents

The same issue as for i-PS should be also pertinent to thermoreversible gelation in crystallizable polymers in general (such as PVC[17], PVA[18], PE[9] and many biopolymers, see earlier) where previously gelation has been attributed exclusively to crystallization, a situation which, as for i-PS, requires reexamination. The scope can be widened further to include liquid crystals, which can also become frequently associated with gelation[20,21]. The issue raised earlier as to what arrests the relevant phase transformation, and thus assures the comparative permanence of the gel remains unanswered, unless it is T_g or chemical inhomogeneities (copolymers) along the chain.

Whatever the phase transition which produces gelation, it will be influenced by the chain conformation. If, say, a new conformation arising on cooling promotes a particular localized phase transition this can then induce gelation. Such a situation has been identified quite recently by Berghmans and coworkers with syndiotactic PMMA[22] and is proposed for the bacterial gellan gum by Atkins[23]. In the former case, the new phase is crystal, while in the latter liquid crystal.

It is not surprising that with all this diversity of gelation effects (and more classes could be quoted) there have been many suggested explanations but no concensus on a unifying scheme. Thus it arises that precedents containing certain features of the present schemes (ref. 10 and this work) can be recognized in the past and current literature. Thus liquid–liquid phase transformation (together with or as an alternative to liquid→crystal transformation) is being quoted for the gelation of isotactic poly(4-methyl-pentene-1)[24], and is stated in a new detailed study on the gelation of poly(n-butyl methacrylate)[25] in both cases, however, without resorting to the, in our opinion, essential role of the glass transition. Also, in addition to phase transformations the concept of the spinodal has also been invoked. The latter was raised in broad general terms for a-PS in CS_2[4] but not followed up when the suggestion of a liquid–liquid phase segregation had been abandoned altogether[3]. More explicitly, a spinodal mechanism has been invoked in connection with gelation

of the more rod-like molecules of gelatin and poly(benzyl glutamate). In the latter case it is given with reference to the liquid–liquid (involving an anisotropic liquid) phase diagram with similarities to our present proposal[26], a work referred to again in connection with gelation–crystallization in i-PS[27]. While acknowledging such precedents where they apply the present study, with that of Arnauts and Berghmans[10], on a thermodynamically well-mapped system of a-PS now provides a firm base from which this diversified subject area can be further pursued.

Design of porous materials

It will be self evident that the present approach to gels offers a route towards planned design of porous materials. It will be apparent that factors such as scale and rigidity of the structure, connectivity and specific morphology should be controllable, based on simple principles underlying gelation. The subject of porosity is receiving widespread attention in other areas without necessarily referring to gelation. There is, for example, the recent work on a-PS yielding morphologies resembling our own[28], or the work leading to rigid foams along chemical routes[29]. Connections of these more colloidal approaches to the creation of porous systems with the present gelation-based route clearly invite exploration.

The issue of connectedness. Definition of a gel

Connectedness is intrinsic to a gel. Previous works implicitly or explicitly envisaged the network elements as entropy elastic, imparting a rubbery character to the gel[1,2]. In some cases this rubbery character was explicitly demonstrated[30], in others merely noted or utilized for producing oriented systems by stretching[2]. The latter was aimed at either obtaining well-oriented X-ray diffraction patterns for crystallographic purposes, or for obtaining technological fibres[19].

Within the framework of the present study, the definition of a physical gel has widened considerably. The previously considered entropy elastic gel is now confined to connectedness arising at the low-concentration side of the phase diagram, irrespective of whether the junctions are constituted by polymer-rich liquid phase or by crystals, or by a combination of the two. At the high-concentration side, the connectedness is provided by a glassy matrix, imparting a glass-like property to the system. Previously such a system may have been considered as a glass which becomes viscoelastic or plasticized above a lowered T_g, rather than a gel. Only occasionally referred to as a gel (xerogel), they were envisaged as a totally different category from the above. We see now that these two distinct systems are generically of the same origin. The same overall glassy character is displayed also at the intermediate concentrations, but nevertheless having a morphology which is distinct from the rest with the strong suggestion of being generated by spinodal decomposition. If so, this would place previous suggestions that spinodal mechanism is responsible for gelation in perspective: without detracting from its intrinsic interest it would only apply to a particular concentration regime, yielding a gel system of a specific bicontinuous morphology within a much broader spectrum of other gel variants. It is hoped that looking at it in this way, the diversity of structures characterized by three-dimensional connectivity, which we now define collectively as gels, can be brought under a common denominator. This approach thus embodies several previously proposed models, each within its range of validity without necessarily one excluding another.

It is then a further important point as to how far there exists a molecular criterion for connectivity which hitherto has been the starting point in most discussion on gels[1]. The criterion of coil overlap should remain pertinent for gels arising at low concentrations, where they are entropy elastic. Yet such a criterion may well need to be modified; it could even be superfluous in the cases where the matrix is a glass. Here phase continuity itself could suffice without any molecular criterion. This would then include the special situation of spinodally generated structures, where such a phase segregation mechanism would be particularly inducive for the formation of bicontinuous gel structures, provided of course that phase segregation is arrested at the suitable stage. As a result, the concept of connectivity is now being invoked in a broadened context embracing either molecular or phase continuity, or both, in what we consider to be a widened definition of physical gels.

ACKNOWLEDGEMENTS

We wish to thank Professor A. Berghmans, Leuven, for interim information communicated to us before publication which substantially benefited the present work. Two of us (RHM and SC) wish to acknowledge support from the Science and Engineering Research Council, and (in the case of SC) also from Edeco Co. Ltd.

REFERENCES

1 Miles, M. J. in 'Developments in Crystalline Polymers' (Ed. D. C. Bassett) Vol. 2, Elsevier, Amsterdam, 1987
2 Keller, A. in 'Structure—Property Relationships of Polymer Solids' (Ed. A. Hiltner) Plenum Press, New York, 1983, p. 25
3 Tan, H., Moet, A., Hiltner, A. and Baer, E. *Macromolecules* 1983, **16**, 28
4 Wellinghoff, S. T., Shaw, J. and Baer, E. *Macromolecules* 1979, **12**, 932
5 Boyer, R. F., Baer, E. and Hiltner, A. *Macromolecules* 1985, **18**, 427
6 Girolamo, M., Keller, A., Miyasaka, K. and Overbergh, N. *J. Polym. Sci., Polym. Phys. Edn.* 1977, **15**, 211
7 Atkins, E. D. T., Isaac, D. H., Keller, A. and Miyasaka, K. *J. Polym. Sci., Polym. Phys. Edn.* 1980, **18**, 71
8 Atkins, E. D. T., Hill, M. J., Jarvis, D. A., Keller, A., Sarhene, E. and Shapiro, J. S. *Colloid Polym. Sci.* 1984, **262**, 22
9 Smith, P. and Lemstra, P. J. *J. Mater. Sci.* 1980, **15**, 505
10 Arnauts, J. and Berghmans, H. *Polym. Commun.* 1987, **28**, 66
11 van Krevelen, D. W. in 'Properties of Polymers', Elsevier, Amsterdam, 1976, p. 383
12 Cahn, J. W. *J. Chem. Phys.* 1965, **42**, 93
13 Feke, G. T. and Prins, W. *Macromolecules* 1974, **7**, 527
14 van Aartsen, J. J. *Eur. Polym. J.* 1970, **6**, 919
15 Odell, J. A., Keller, A. and Miles, M. J. *Polymer* 1985, **26**, 1219
16 Keller, A., Müller, A. and Odell, J. A. *Prog. Colloid Polym. Sci.* 1987, **75**, 179
17 Guerrero, S. J., Keller, A., Soni, P. L. and Geil, P. H. *J. Polym. Sci., Polym. Phys. Edn.* 1980, **18**, 1533
18 Berghmans, H. and Stoks, W. in 'Interpretation of Fundamental Polymer Science and Technology' (Eds. L. A. Kleintjens and P. J. Lemstra) Elsevier, London, 1986, p. 218
19 Barham, P. J. and Keller, A. *J. Mater. Sci.* 1985, **20**, 2281
20 Tsowladze, G. and Skoulios, A. *J. Chim. Phys.* 1963, **60**, 626
21 Grosius, P., Gallot, Y. and Skoulios, A. *Makromol. Chem.* 1970, **132**, 35
22 Berghmans, H., Dankers, A., Frency, L., Stoks, W., De Schryver, F. E., Moldenaers, P. and Mavis, J. *Polymer* 1987, **28**, 97

23 Atkins, E. D. T. *Int. J. Biol. Macromol.* 1986, **8**, 323
24 Tanigami, T., Susuki, H., Yamoura, K. and Matsuzana, S. *Macromolecules* 1985, **18**, 2595
25 Wolf, B. A. *et al. Macromolecules* submitted
26 Miller, W. G., Kow, L., Tohyama, K. and Voltaggio, V. *J. Polym. Sci., Polym. Symp.* 1978, **65**, 91
27 Guenet, J. M. *Macromolecules* 1985, **18**, 420
28 Aubert, J. H. and Clough, R. L. *Polymer* 1985, **26**, 2047
29 Litt, M. H., Msiem, B. R., Krieger, M., Chien, T. T. and Lu, H. L. *J. Colloid Interface Sci.* 1987, **115** (2), 312
30 Koltisko, B., Keller, A., Litt, M., Baer, E. and Hiltner, A. *Macromolecules* 1986, **19**, 1207